A METHODOLOGY FOR FLOTATION DEINKING MODEL VALIDATION

Project F00903

Report 7

to the

MEMBER COMPANIES OF THE INSTITUTE OF PAPER SCIENCE AND TECHNOLOGY

July 1998

INSTITUTE OF PAPER SCIENCE AND TECHNOLOGY

Atlanta, Georgia

A METHODOLOGY FOR FLOTATION DEINKING MODEL VARIATION

Project F00903

Report 7

A Progress Report

to the

MEMBER COMPANIES OF THE INSTITUTE OF PAPER SCIENCE AND TECHNOLOGY

By

K.S. Maruvada and T.J. Heindel

July 1998

TABLE OF CONTENTS

1 Executive Summary

A two-parameter population balance-type kinetic model has been proposed earlier for the flotation of ink particles from a suspension containing recycled cellulose fibers. In this report, a validation scheme for the above model is presented. Experiments are outlined that will be conducted using a bench top flotation column in a semi-batch manner to validate this model. In order to interpret the experimental data, the global model equations are rewritten to suit the current experimental conditions. These equations, which determine the concentration of free ink particles in the suspension, are found to be non-linear. Hence, two special cases are considered whose solutions have been *analytically* determined.

The first special case assumes that the gas holdup (percent gas by volume) is less than 10%. Experimental data can be fitted to this case to determine the forward rate constant k_1, which is a measure of the overall probability of the formation of a stable bubble/particle aggregate. The second special case is applicable at the beginning of flotation experiment where less than 10% of the particles have been removed. Experimental data can be fitted to this case to quantify the reverse rate constant k_2, a measure of bubble/particle aggregate destruction.

The information outlined in this report will be used to experimentally determine k_1 and k_2, which will then be compared to model predictions. Model improvements may also be identified from these results. The next step after laboratory model validation will be pilot plant and mill-scale model validation.

2 Introduction

Flotation is commonly being used in the paper industry to remove hydrophobic contaminants such as ink particles and stickies from a suspension containing recycled cellulose fibers [1-4]. Despite being commonly used, the mechanism of ink particle capture by air bubbles is not completely understood. Recent emphasis by several investigators [5-9] on the fundamental aspects of the air bubble - ink particle interactions has provided a much clearer understanding of the particle capture phenomena. Nonetheless, the current level of understanding is far from sufficient for developing commercial deinking processes which run under optimum operating conditions.

The overall flotation deinking process is based on the common assumption that it comprises a series of microprocesses that must occur sequentially to achieve successful particle removal. These microprocesses involve capture (collision) of the particle by the bubble, attachment of the particle to the bubble as it slides over the bubble surface, the creation of a three-phase contact, and the stabilization of the bubble/particle aggregate as it rises through the suspension. Each of these microprocesses has associated with it a probability that it will successfully occur, which is a function of the bubble and particle physical properties (e.g., diameter, density), the fluid properties (e.g., viscosity, surface tension), and the system properties (e.g., contact angle, turbulent energy density). Based on mineral flotation experimental evidence, the flotation process is thought to be analogous to a chemical reaction between air bubbles and ink particles leading to the formation of aggregates [10].

Recently, a two-parameter population balance-type kinetic model has been proposed by the authors in [11-13] to predict the efficiency of flotation deinking of recycled paper pulp. This model uses a reversible elementary chemical reaction analogy to describe the interactions between air bubbles and free ink particles, which result in the formation of bubble/particle aggregates. The rate constant associated with the formation of a stable bubble/particle aggregate is referred to as the forward rate constant of the reaction k_1, and the rate constant associated with the destabilization of the aggregate is referred to as the reverse rate constant k_2. These rate constants depend on the probabilities of the various microprocesses which further depend on various system parameters. An elaborate discussion on these rate constants is provided in Section 3.3.3.

The objective of this report is to explore and bridge the gap between the generalized flotation deinking model proposed by the authors in [11-13], its validation aspects, and scale up related issues. This is accomplished by focusing attention on a semi-batch flotation deinking process, which can be easily studied using a bench top experimental setup.

3 Model Validation Methodology

3.1 Experimental Apparatus

The experimental apparatus consists of a column into which a desired furnish is loaded. This column contains either a sparger or an orifice plate at the bottom for air supply. Air at a known volumetric flow rate (Q), is bubbled through the suspension containing the recycled cellulose fibers and ink particles. It is assumed that air bubbles that are formed at the bottom of the column rise through the suspension at their terminal

rise velocity. Bubble coalescence is also assumed to be negligible. The size of the air bubble is controlled either by changing the orifice diameter or sparger type. The entire bubble surface is assumed to be rigid because of the presence of surface active substances [14]. This is a valid assumption as long as the bubble size is small. The proposed flotation experiments will be carried out in a semi-batch manner in which a fixed volume of the pulp suspension will be used while air is continuously injected. Figure 1 is a schematic of the experimental system. The mixture volume (including stock and gas) in a steady state situation will be denoted by V. The agitator provides the necessary agitation.

3.2 Model Description

In this section, the equations governing the population of the number of ink particles (both free and total number) in the system are presented. The number of bubbles in the column can be calculated by measuring the gas holdup (gas percent by volume) and the size of a single bubble assuming all bubbles are of a uniform size. Let n_B denote the total number of bubbles per unit volume in the column at any given time. The total number of bubbles consists of bubbles free of particles and those with particles attached to them. Both free bubbles (n_B^f) and bubbles with particles attached (n_B^a) are functions of time, while the total number of bubbles is a constant at any given instant of time.

$$n_B = n_B^f(t) + n_B^a(t) \tag{1}$$

If V_B is the volume of a single bubble, then the total number of air bubbles entering the column per unit time is given by the following expression.

$$\dot{n}_B = \frac{Q}{\mathrm{V}_B} \tag{2}$$

Where Q is the known volumetric flow rate. If υ_B is the terminal rise velocity of the bubble, then the residence time of the air bubble inside the column is given by H/υ_B, where H is the height of the contents inside the column (Figure 1). Therefore the total number of bubbles in the column at any time is given by

$$N_B = \frac{Q}{\mathrm{V}_B}\frac{H}{\upsilon_B} \tag{3}$$

Hence the concentration of air bubbles per unit volume is

$$n_B = \frac{Q}{\mathrm{V}_B}\frac{H}{\upsilon_B}\frac{1}{V} \tag{4}$$

Here V is the reactor volume (i.e., the volume of stock and gas). Notice that n_B is a constant when the volumetric flow rate is fixed and it is inversely proportional to the cross-sectional area of the column (V/H). Hence, for a given flow rate and bubble size, the number density of bubbles (n_B) is inversely proportional to the cross-sectional area of the column.

3.2.1 Balance Equations

Under steady-state operation, the total number of bubbles entering the column is identical to the total number of bubbles leaving the column, assuming negligible bubble coalescence. Although this assumption is very stringent, it will be relaxed in future studies so that a distribution of bubble sizes can be considered. In other words, it is a steady-state process with respect to the air bubbles. Let n_B^a/n_B denote the fraction of bubbles with particles attached inside the column. Since the contents are assumed to be

well mixed, the same fraction also represents the fraction of bubbles with attached particles in the exit stream. Assuming that each bubble with attached particles is carrying only one ink particle, the number of ink particles leaving the column can be calculated by multiplying this fraction with the total number of bubbles leaving the column. Hence the rate of decrease of the ink particles inside the column is given by the following balance equation.

$$V\frac{dn_p}{dt} = -\frac{Q}{V_B n_B}\left(n_p - n_p^f\right) \tag{5}$$

Where n_p and n_p^f are the total number of particles per unit volume and the number of free particles available to attach to free bubbles, respectively. Observe that in the above equation, both n_p and n_p^f are functions of time. Similarly, another balance equation can be written for the number of free particles inside the column. It should be noted that no free ink particles are either entering or leaving the column and they are only participating in the formation of bubble/particle aggregates. Using our reaction model previously detailed in [11-13], the balance equation for the free ink particles can be written as follows.

$$\frac{dn_p^f}{dt} = -k_1 n_p^f n_B^f + k_2 n_B^a \tag{6}$$

Here k_1 and k_2 are the rate constants for the forward and reverse reactions, respectively. These two constants depend upon the various microprocess probabilities that comprise the mechanism of bubble/particle aggregate formation and destruction. As previously stated, these two parameters are functions of the bubble, particle, fluid, and system

properties. They apparently do not depend upon the population density of the ink particles or the air bubbles in the system. Equation (6) can be rewritten in terms of n_p^f as given below.

$$\frac{dn_p^f}{dt} = -k_1 n_p^f n_B + k_1 n_p^f \left(n_p - n_p^f\right) + k_2\left(n_p - n_p^f\right) \tag{7}$$

Equations (5) and (7) are coupled with each other and are solved simultaneously, subject to the initial condition that $n_p = n_p^f = n_{po}^f$. Where n_{po}^f is the number density of ink particles at time t = 0. To simplify the solution procedure, the governing equations are non-dimensionalized as given below.

$$n_p, n_p^f \sim n_{po}^f \qquad k_1 \sim \left(t^* n_{po}^f\right)^{-1}$$

$$t \sim t^*\left(= H/\upsilon_B\right) \qquad k_2 \sim \left(t^*\right)^{-1}$$

Here t^* is the residence time of a single bubble in the column. Hence it is the time taken for a single bubble to rise to the froth layer at the top. Once it reaches the froth layer, it is assumed to be removed from the system. The new dimensionless variables are as given below.

$$\alpha = n_p / n_{po}^f \,,\ \gamma = n_p^f / n_{po}^f \qquad \tilde{k_1} = k_1 t^* n_{po}^f$$

$$\tilde{t} = t/t^* \qquad \tilde{k_2} = k_2 t^*$$

Using the above scheme the two governing equations, with the accompanying boundary conditions, are scaled and rewritten as follows.

$$\varepsilon_p \alpha' = -(\alpha - \gamma) \qquad \alpha(\tilde{t} = 0) = 1 \tag{8}$$

$$\gamma' = -\tilde{k}_1 E\, \gamma + \tilde{k}_1 \gamma(\alpha - \gamma) + \tilde{k}_2(\alpha - \gamma) \qquad \gamma(\tilde{t} = 0) = 1 \tag{9}$$

Here the prime indicates total differentiation with respect to dimensionless time. The two parameters that appear in the scaled equations are $\varepsilon_p = V_B n_B$ and $E = n_B / n_{po}^f$ where ε_p is the gas holdup per unit volume and E is a measure of the relative bubble population with respect to the initial number of ink particles. The above two equations can be combined to result in a single differential equation for the number density of total particles (α) as given below.

$$\tilde{k}_1 \varepsilon_p^2 (\alpha')^2 + \varepsilon_p \alpha'' + \left(1 + \tilde{k}_2 \varepsilon_p + \tilde{k}_1 E \varepsilon_p\right) \alpha' + \tilde{k}_1 \varepsilon_p (\alpha \alpha') + \tilde{k}_1 E \alpha = 0 \tag{10}$$

At $t > 0$, α represents the total number of particles in the system. After a flotation experiment is completed, the number of particles in the system (the accepts) are assumed to be all free particles (i.e., $\alpha = \gamma$). Equation (10) is a second order differential equation containing two nonlinear terms. An exact solution to this equation has to be obtained numerically. However, in the context of model validation, analytical progress can be made if we consider the following two special cases.

The first special case assumes that the gas holdup is less than 10% and therefore the magnitude of ε_p is always less than 0.1. Experimental data can be fitted to this case to determine the forward rate constant k_1, which is a measure of the overall probability of the formation of a stable bubble/particle aggregate. The second special case is applicable at the beginning of flotation experiment where less than 10% of the particles have been

removed. Experimental data can be fitted to this case to quantify the reverse rate constant k_2, a measure of bubble/particle destruction.

3.2.2 Solution for Low Gas Holdup

When the gas holdup is small, the following simplifications can be made to Equation (10). Since the particle concentration is made dimensionless by dividing with the initial concentration, its value is always less than one. The dimensionless time derivative of α can at most be an order one quantity. So, when a small parameter such as ε_p multiplies an order one quantity, the contribution due to that particular term is decreased by at least one order of magnitude. Under this argument, to obtain a leading order solution, it is safe to drop the terms containing ε_p. In doing so, the term containing the highest order derivative in Equation (10) is also lost resulting in the following first order differential equation.

$$\alpha' + \tilde{k_1} E \alpha = 0 \tag{11}$$

The solution to this simplified problem is expected to deviate from the exact solution only in the small neighborhood of $t = 0$. Because of the decrease in the order of the differential equation, one of the initial conditions has to be sacrificed. Equation (11) can be solved subject to the initial condition on α (i.e., $\alpha = 1$ when $t = 0$) which results in an exponential decrease in the number density of the ink particles. In the dimensional form, the result is

$$n_p = n_p^f = n_{po}^f \, e^{-k_1 n_B t} \tag{12}$$

This solution, which is a straight line on a semi-log scale, is plotted in Figure 2. The slope of the straight line is negative and the magnitude is $k_1 n_B$. It is valid for all times except near $t = 0$. This is different from the traditional solution in the following manner. In this solution the effect of bubble population is isolated from the effect of the rate constant associated with the particle capture, thereby enabling us to study their effects independently. Notice that increasing either k_1 or n_B contributes to an increase in the particle removal rate.

3.2.3 Short Time Solution

In Equation (10), the two nonlinear terms can be linearized about their initial values using a Taylor-Series expansion. The resulting equation is a second order linear ordinary differential equation with constant coefficients which is given by

$$\varepsilon_p \alpha'' + \left[1 + \left(\tilde{k}_2 + \tilde{k}_1\right)\varepsilon_p + \tilde{k}_1 E \varepsilon_p\right]\alpha' + \tilde{k}_1 E \alpha = 0 \tag{13}$$

The solution to this equation is

$$\alpha(t) = \frac{1}{m_2 - m_1}\left[m_2 e^{m_1 t} - m_1 e^{m_2 t}\right] \tag{14}$$

$$\gamma(t) = \frac{1}{m_2 - m_1}\left[\alpha(t) + \varepsilon_p m_1 m_2 \left(e^{m_1 t} - e^{m_2 t}\right)\right] \tag{15}$$

Here m_1 and m_2 are the roots of the quadratic characteristic equation both of which are negative real numbers corresponding to the second order differential equation above (Eq. (13)). This solution can be considered valid for short times (i.e., while $0.9 \le \alpha, \gamma \le 1.0$). In order to plot this solution, the ranges for the parameters need to be determined. Table 1 presents the typical values for the various parameters used in this study.

Figure 3 is a plot of the dimensionless particle concentration in the accepts as a function of dimensionless time. This figure indicates that the number of particles attached to bubbles ($n_p^a = n_p - n_p^f$) can be significant in the beginning of the flotation experiment. Since k_2 depicts a measure of the instability of these bubble/particle aggregates, the short time solution may in fact provide an opportunity to determine its magnitude. The actual behavior of these two curves depends on the values of the input parameters pertinent to the problem. Although these two curves deviate from each other in the beginning, they eventually have to collapse to become a single curve and asymptotically approach a constant value, which may be non-zero, at sufficiently long times. In order to study the dependence of various process variables on the short time solution, a reasonable estimate for the input parameters must be specified. Since estimates for k_2 are not known, it would be appropriate to undertake this study once the data from our preliminary experiments become available.

In Figure 4, the dimensionless free particle concentration of ink particles in the accepts is plotted as a function of dimensionless time. Dimensional time can be obtained by multiplying bubble residence time by the dimensionless time. In this figure, a comparison is made between the short time solution obtained by solving Eq. (13) and the exponential solution obtained by solving Eq. (11). It can be easily seen that the exponential solution over estimates the number of ink particles in the accepts during the initial flotation period.

The overall findings of this section may be summarized as follows. Typically, the results of a flotation deinking experiment may be plotted as the number of ink particles in

the accepts as a function of time. By analyzing the trend after the initial time (i.e., while $0.1 \leq \gamma \leq 0.9$), the value of the forward rate constant k_1 can be determined. Once k_1 is known, the short time trend (i.e., while $0.9 \leq \gamma \leq 1.0$) can be analyzed to determine the reverse rate constant k_2. The above mentioned methodology is a means to experimentally determine the two parameters of the model.

3.3 Parameter Estimation

In the following section, a discussion is provided on the two independent variables n_B and n_{po}^f along with the rate constants which depend on the microprocesses.

3.3.1 Number Density of Bubbles (n_B)

As evident from Equation (4), for a constant volume of the pulp suspension, the bubble density can easily be increased experimentally by one of two methods. Either by increasing the volumetric flow rate of the gas or by decreasing the cross-sectional area of the flotation column. When the volumetric flow rate is increased, the dynamic surface tension can be higher than its equilibrium value which changes the bubble size and therefore k_1. However, if the surfactant concentration is sufficiently high so that a local depletion does not arise, then the surface tension remains constant at its equilibrium value. Decreasing the cross-sectional area while maintaining the volume of the column constant increases the number density of bubbles without changing the bubble size. Hence, a slender column is preferable to a wider one. In the case of a continuous process, this increases the pressure drop suggesting an optimum value for the column diameter. It

is interesting to note that the flotation efficiency depends on the geometry of the column. However, the model equations presented here are applicable to various geometries.

This solution is not very accurate for very short times because of the reduction in the order of the governing differential equation (Eq. 10). Hence, instead of a zero slope for α at time $t = 0$, a finite slope is present. However, the behavior at later times can be accurately represented by this solution. Therefore this result can be used to experimentally determine the value of the forward rate constant k_1, once the number density of the bubbles (n_B) is known. An order of magnitude argument suggests that the assumption of ε_p being small is valid as long as the gas holdup is less than 10% of the total mixture volume. In most cases, this is typically applicable.

Assuming that the gas holdup in the experimental conditions of Vidotti et al. [15] is small, their data have been analyzed in light of our model. In their experimental studies, white office paper has been printed upon using four different toners (HP3 Laser Printer, HP4 Laser Printer, Canon Copier, and Toshiba Copier) before it was repulped under standard conditions and flotation experiments were carried out. Their findings from the flotation experiments have been tabulated as the number of ink particles remaining in the accepts as a function of time. The present study uses their experimental data and for each particle size range, this data is plotted as a function of time. The data points at time $t = 0$ have been omitted for reasons mentioned in Section 3.2.2. An exponential curve is fitted to the experimental data and the coefficient, exponent, and goodness of fit parameter (R^2) have been obtained for each particle size range. The values are presented in Table 2. The following observations may be made from this data. The exponent ($k_1 n_B$)

ranges from 0.01 to 0.05. Since the number density of the bubbles for this experiment is not known, the magnitude of k_1 can not be estimated. It is interesting to note that this value is nearly a constant and does not vary over a wide range. Since n_B is not expected to be different among these experiments, the observed variation in $k_1 n_B$ may be coming from the variation in k_1 as the particle size changes. Despite the aforementioned assumptions, an exponential fit provides a good fit for the experimental data as indicated by R^2 values.

3.3.2 Initial Particle Concentration (n_{po}^f)

When a printed paper is repulped, the ink is broken down into particles typically ranging in sizes between 10 and 500 microns. In fact there is a distribution of these particle sizes over the entire range. While most of these particles are completely detached from cellulose fibers, some of them remain embedded in a network of fibers. In such cases, the ink particles appear to have fibers sticking out from them. In the literature, these particles are referred to as hairy particles [16]. The behavior of these particles during the flotation process is not clearly known. The mathematical model for flotation deinking has several assumptions one of them being the absence of hairy particles. Hence, for validation purposes, our preliminary experiments will not contain hairy particles in the recycled pulp suspension. Fused ink particles will be prepared separately and added to a white office paper pulp suspension which will be used for our preliminary flotation experiments.

The following procedure is adopted from Vidotti et al. [17] for preparing fused ink particles. A known set of characters will be printed on a cellophane sheet. The

cellophane sheet will be soaked in water for a few hours and the printed characters will be stripped off the sheet by gentle mechanical agitation. The cellophane sheets are removed and rinsed off to remove any characters still adhering to it. The water solution containing detached ink characters will be placed in a disintegrator and subjected to conditions prevailing for repulping of the paper. Once completed, the solution containing flakes of ink particles will be filtered to remove water. All the ink particles will be collected in the funnel and dried under constant humidity conditions. Dried ink particles will then be analyzed using image analysis and their particle size distribution will be obtained from a representative sample of the fused ink particles.

As mentioned earlier, the initial condition used in solving Eq. (5) and Eq. (7) is the concentration of ink particles in the flotation cell at time $t = 0$. The ensuing procedure outlines the steps in determining the initial concentration of the ink particles. The size range of the ink particles is divided into n bins. For each bin the mean diameter of the particles is d_i and their mean planform area is A_i. A knowledge of the size distribution of the fused ink particles allows us to determine the fraction, f_i , of the total number of ink particles belonging to each bin.

It is reasonable to assume that all the ink particles have a uniform thickness, t_p, which can be determined by microscopic examination of printed paper. If N_p represents the total number of particles present in the flotation column, then the weight of the ink particles added can be given by

$$w = \rho_p \sum_{i=1}^{n} N_p f_i A_i t_p \tag{16}$$

Hence, by knowing the size distribution, average thickness, and the weight added, the total number of ink particles, N_p, in the suspension can be estimated. Once this is known, the initial concentration of ink particles can be obtained by

$$n_{po}^{f} = \frac{N_p}{V} \tag{17}$$

This estimate will be used for plotting the short time solution presented in the previous section.

3.3.3 Rate Constants

In this section, a procedure to theoretically estimate the rate constants is explained. As described in the introduction, the forward rate constant k_1 and the reverse rate constant k_2 depend upon the various microprocess probabilities that constitute the bubble/particle aggregate formation and its subsequent stability behavior. Extensive research is being carried out to accurately predict these microprocess probabilities. In this section a brief review of the various microprocesses and their probabilities is presented. The first step in the aggregate formation is referred to as the capture (or collision) of the ink particle present in the so-called streaming tube that corresponds to a given bubble trajectory, and has an associated probability, P_c. Once an ink particle has been successfully intercepted by a rising air bubble, it then enters a thin film region that surrounds the bubble in which it slides along the contour of the bubble surface. During the sliding process, the thin film that separates the ink particle from the air bubble gradually thins. There is a finite probability that the film will become sufficiently thin so that the surface forces such as electrostatic and dispersion forces become important. This probability is called the probability of adhesion by sliding (P_{asl}). The third step in the

aggregate formation is the formation of a stable three-phase contact line, with an associated probability P_{tpc}. Typically, this step is not assumed to be a limiting one and its probability is assumed to be close to one. Finally once the particle/bubble aggregate has formed, the probability that it remains stable is given by P_{stab}. The detailed mathematical expressions for these probabilities have been given in [13, 18, 19]. Hence, to avoid repetition, they are not mentioned here. The overall probability for the successful formation of a bubble/particle aggregate is obtained as given below.

$$P_{overall} = P_c P_{asl} P_{tpc} P_{stab} \tag{18}$$

The kinetic constants k_1 and k_2 are positive numbers described by the various microprocess probabilities and the collision frequency:

$$k_1 = Z P_{overall} \tag{19}$$

$$k_2 = Z' P_{destab} = Z'\left(1 - P_{stab}\right) \tag{20}$$

In Eq. (19), Z is the collision frequency which we take to have the form implied by the work of Liepe and Möckel [20], namely,

$$Z = 2^{7/9}\frac{5}{3}\left(\frac{\varepsilon^{4/9}}{\nu_l^{1/3}\rho_l^{2/3}}\right)\left(R_p + R_B\right)^2 \times \left(R_p^{14/9}\Delta\rho_p^{4/3} + R_B^{14/9}\Delta\rho_B^{4/3}\right)^{1/2} \tag{21}$$

where ν_l and ρ_l are the fluid kinematic viscosity and fluid density, respectively, ε is the turbulent energy density, R_p and R_B are the particle and bubble radius, $\Delta\rho_p = \rho_p - \rho_l$, $\Delta\rho_B = \rho_B - \rho_l$, and ρ_p and ρ_B are the particle and bubble density, respectively. Equation (21) would be applicable to flotation cells with agitation. Note that this expression differs from that presented in [13] by a factor of $n_B n_p$, where n_B and n_p are the total number of

bubbles and particles per unit volume, respectively. The original expression in [13] was adopted following the work of Schulze [9]. However, as recently pointed out by Julien Saint Amand [7], the Z in Eq. (19) should not have the $n_B n_p$ term because it accounts for the collisions between free particles (n_p^f) and free bubbles (n_B^f), which are already incorporated into Eq. (6). Therefore, $Zn_p^f n_B^f$ is a true collision frequency with units of number per unit time per unit volume.

Based on new research, k_2 in Eq. (20) is slightly different from that previously presented (i.e., [13]). Based on dimensional considerations, k_2 should have units of 1/time, giving the second term on the right-hand side of Eq. (6) the units of number per unit time per unit volume, which is consistent with the other terms. Since P_{destab} (= 1-P_{stab}) is a true probability and is unitless, an additional term has to be included in k_2, which we call Z' and has units of 1/time. This term could be thought of as a collision rate between bubble/particle aggregates and the "thing" that makes the aggregate unstable, like a turbulent eddy. Current research is directed toward quantifying this term.

As a first estimate, we argue that $k_2 \leq 1$, based on the reasoning that at most, the number of free particles that could be generated at a given instant in time due to the destabilization of the bubble/particle aggregate is equivalent to n_B^a, the number of bubbles per unit volume with attached particles at that instant in time. This assumes that only one particle could attach to a bubble, an assumption we are currently relaxing. Therefore, values of $k_2 > 1$ have no physical meaning. As a first approximation, we will

assume that $Z' = 1$ (and has the appropriate units of 1/time). This assumption will be modified as we continue to research this area.

Figure 5 presents the behavior of the overall probability of formation of a stable bubble/particle aggregate as a function of particle size for various bubble sizes. The following values have been used in plotting Figure 5 (turbulent energy density = 2.0 W/kg, particle density = 1.3 g/cm^3, contact angle = 60°, surface tension = 50 dynes/cm). The result indicates that for each bubble size, there is an optimum particle size where the overall probability is maximized. As the bubble size increases, the optimum particle size also increases suggesting that small bubbles are preferable for removing small ink particles and large bubbles are preferred for the large particles. Typically, recycled pulp suspensions contain ink particles that cover a wide size distribution from less than 10 μm in diameter for flexographic inks to more than 500 μm in diameter for toner particles. Hence for such a pulp suspension containing a distribution of particle sizes, a corresponding distribution of bubble sizes would be an optimum choice.

Figure 6 presents the probability of destabilization which is related to the reverse rate constant k_2. As evident, the probability varies over several orders of magnitude. For a given bubble size, the probability remains very small until the particle size reaches a threshold value beyond which the probability becomes significant. This suggests that for a given bubble size, as the particle size increases, the aggregate becomes unstable.

As indicated in Figure 5, for any given bubble size there is an optimum particle size for which the probability of aggregate formation is highest. Figure 7 presents the relationship between particle radius and bubble radius for which the overall probability of

bubble/particle aggregate formation is maximum. In the absence of an aggregate destabilization mechanism, such as the absence of turbulent eddies or so in the system, this curve represents the optimum bubble radii required to capture a given distribution of particle sizes. The observed discontinuity is due to the transition from Stokes flow regime to a non-Stokes flow regime as the particle radius increases (e.g., see [19]). These curves are plotted for three different values of the particle density and as expected, the transition occurs at different values of the particle radius.

4 Conclusions

A methodology to validate the flotation deinking model is presented. The two kinetic parameters of the model can be experimentally determined by analyzing the number density of the ink particles in the flotation accepts as a function of time. The forward rate constant k_1 can be determined by fitting an exponential curve to the experimental data while $0.1 \le \gamma \le 0.9$. Once k_1 is determined, k_2 can be determined from the short time solution (i.e., while $0.9 \le \gamma \le 1.0$). Experimental values for the kinetic parameters can then be compared with the theoretical predictions.

5 References

1. Ortner, H.E., *Recycling of Papermaking Fibers: Flotation Deinking*, TAPPI Press, Atlanta, GA, 1981.

2. Fallows, J.D., "Flotation Deinking," *Deinking Seminar (Atlanta) Notes*, Atlanta, GA, TAPPI Press (June 22-24, 1992).

3. McCool, M.A., "Flotation Deiniking," *Secondary Fiber Recycling*, R.J. Spangenberg, Ed., Atlanta, GA, TAPPI Press, 141-162 (1993).

4. Ferguson, L.D., "Flotation Deinking Technology," *1995 Deinking Short Course*, Vancouver, WA, TAPPI Press, Chapter 10 (June 4-7, 1995).

5. Schulze, H.J., *Physico-Chemical Elementary Processes in Flotation*, Elsevier, Berlin, 1984.

6. Ahmed N., and Jameson, G.J., "Flotation Kinetics," *Mineral Processing and Extractive Metallurgy Review*, **5**: 77-99 (1989).

7. Julien Saint Amand, F., "Hydrodynamics of Flotation: Experimental Studies and Theoretical Analysis," *1997 TAPPI Recycling Symposium*, Atlanta, GA, TAPPI Press, 219-241 (1997).

8. Thompson E.V., "Review of Flotation Research by the Cooperative Recycled Fiber Studies Program, Department of Chemical Engineering, University of Maine," *Paper Recycling Challenge Vol. II - Deinking & Bleaching*, R. Doshi and J.M Dyer, Eds., Doshi & Associates Inc., Appelton, WI, 31-68, 1997.

9. Schulze, H.J., "The Fundamentals of Flotation Deinking in Comparison to Mineral Flotation," *1st Research Forum on Recycling,* Toronto, Ontario 161-167 (October 29-31, 1991).

10. Gochin, R.J., "Flotation," *Solid-Liquid Separation*, L. Svarovsky, Ed., London, Butterworths, 591-613 (1990).

11. Bloom, F., and Heindel, T.J., "Mathematical Modelling of the Flotation Deinking Process," *Mathl. Comput. Modelling*, **25**(5): 13-58 (1997).

12. Bloom, F., and Heindel, T.J., "Mathematical Modelling of Flotation Deinking Efficiency," *Journal of Colloid and Interface Science* **190**: 182-197 (1997).

13. Heindel, T.J., and Bloom, F., "New Measures for Maximizing Ink Particle Removal in a Flotation Cell," *1997 TAPPI Recycling Symposium*, Atlanta, GA, TAPPI Press, 101-113 (1997).

14. Davis, R.E., and Acrivos, A., "The Influence of Surfactants on the Creeping Motion of Bubbles," *Chem. Eng. Sci.*, **21**, 681-685 (1966).

15. Vidotti, R.M., Johnson, D.A., and Thompson, E.V., "Repulping and Flotation Studies of Photocopied and Laser-printed Office Paper: Part - II," *Progress in Paper Recycling,* **3**(3): 39-49 (1994).

16. Johnson, D.A., and Thompson, E.V., "Fiber and Toner Detachment During Repulping of Mixed Office Waste Containing Photocopied and Laser-printed Paper," *TAPPI Journal*, **78**(2): 41-46, 1995.

17. Vidotti, R.M., Johnson, D.A., and Thompson, E.V., "Visual Observations of Bubble/Particle Interactions," *4th Research Forum on Recycling*, 39-46, October 1997.

18. Heindel, T.J., and Bloom, F., "Mathematical Modelling of the Overall Flotation Deinking Process: Probability of Collision Improvements," Report 4, Project F00903, IPST, Atlanta, GA., 1998.

19. Heindel, T.J., and Bloom, F., "Mathematical Modelling of the Overall Flotation Deinking Process: Probability of Attachment by Sliding Improvements," Report 6, Project F00903, IPST, Atlanta, GA., 1998.

20. Liepe, F., and Möckel, O.H., "Untersuchengen zum Stoffvereinigen in flüssiger Phase," *Chemical Technology*, **30**: 205-209 (1976).

6 Nomenclature

A_i	Average area of the particles belonging to bin *i*
d_i	Average planform diameter of the particles belonging to bin *i*
E	Relative bubble population with respect to the initial number of particles
f_i	Fraction of ink particles belonging to bin *i*
H	Height of flotation column contents (stock and gas)
k_1	Forward reaction rate constant
k_2	Reverse reaction rate constant
m_1	First root of the characteristic equation corresponding to Equation (13)
m_2	Second root of the characteristic equation corresponding to Equation (13)
N_B	Total number of bubbles present in the column under steady conditions
n_B	Number of bubbles per unit volume
n_B^a	Number of bubbles attached to ink particles per unit volume
n_B^f	Number of unattached (free) bubbles per unit volume
N_p	Total number of ink particles added to the pulp suspension
n_p	Total number of particles per unit volume
n_p^a	Number of particles attached to air bubbles per unit volume
n_p^f	Number of free particles per unit volume
n_{po}^f	Concentration of free particles in the suspension at time $t = 0$
P_c	Probability of capture of the particle by the air bubble
P_{asl}	Probability of adhesion by sliding
P_{tpc}	Probability of the formation of a three-phase contact line
P_{stab}	Probability that the bubble/particle aggregate remains stable
$P_{overall}$	Overall probability of a stable bubble/particle aggregate formation
Q	Volumetric gas flow rate
R_B	Radius of the air bubble

t_p	Average thickness of the fused ink particles
t	Flotation time in seconds
t^*	Residence time of a single bubble inside the column
υ_B	Terminal rise velocity of the air bubble in the suspension
V	Volume of the stock and gas
V_B	Volume of a single air bubble
w	Weight of the fused ink particles added to pulp
Z	Collision frequency of the air bubble with particles
Z'	Frequency of bubble/particle aggregate exposure to destabilizing conditions
α	Normalized concentration of total particles (both free and attached)
γ	Normalized concentration of free particles
ρ_p	Density of the fused toner particles
ε_p	Porosity of the mixture; $V_B n_B$
‘	Superscript used to denote differentiation with respect to non-dimensional time
~	Superscript used to denote dimensionless variables

7 Tables

Table 1. Typical values for the parameters used in this study.

Parameter /Variable	Symbol	Range used in this study
Gas holdup	ε_p	0 - 0.1
Gas flow rate (cm^3/s)	Q	10^{-4} - 10^{1}
Bubble size (mm)	R_B	0.2 - 2.0
Number density of bubbles ($\#/cm^3$)	n_B	10^{-3}-10^{1}
Number density of particles ($\#/cm^3$)	n_{po}^f	10^{1} - 10^{4}

Table 2. Regression results for the experimental data of Vidotti et al. [15].

R_p	HP3-LP			HP4-LP		
Microns	*Coeff.*	$k_1 n_B$	R^2	*Coeff.*	$k_1 n_B$	R^2
75	0.2003	0.0450	0.9857	0.2180	0.0213	0.9353
100	0.1465	0.0378	0.9058	0.1879	0.0196	0.9781
125	0.2047	0.0521	0.9921	0.1885	0.0199	0.9573
150	0.1868	0.0454	0.9598	0.2307	0.0248	0.9734
175	0.2140	0.0375	0.7846	0.2832	0.0316	0.9849
200	0.2310	0.0394	0.9029	0.3102	0.0328	0.9919
225	0.2904	0.0458	0.8377	0.3710	0.0357	0.9662
250	0.3734	0.0475	0.9230	0.3719	0.0323	0.9886
R_p	Canon Copier			Toshiba Copier		
Microns	*Coeff.*	$k_1 n_B$	R^2	*Coeff.*	$k_1 n_B$	R^2
75	0.4213	0.0271	0.9346	0.2404	0.0286	0.9789
100	0.3745	0.0282	0.9980	0.2347	0.0287	0.9938
125	0.3531	0.0293	0.9197	0.2758	0.0332	0.9496
150	0.3045	0.0257	0.9848	0.2867	0.0341	0.9767
175	0.3202	0.0402	0.8584	0.2900	0.0299	0.8570
200	0.3228	0.0335	0.9107	0.3471	0.0345	0.9698
225	0.4399	0.0428	0.9899	0.3472	0.0353	0.9548
250	0.4524	0.0254	0.9203	0.4579	0.0278	0.9999

8 Figures

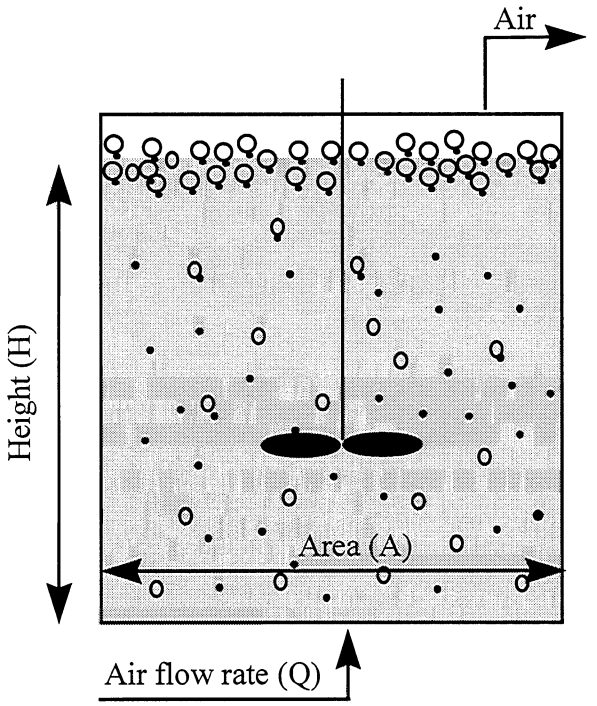

Figure 1: Schematic of the flotation deinking cell.

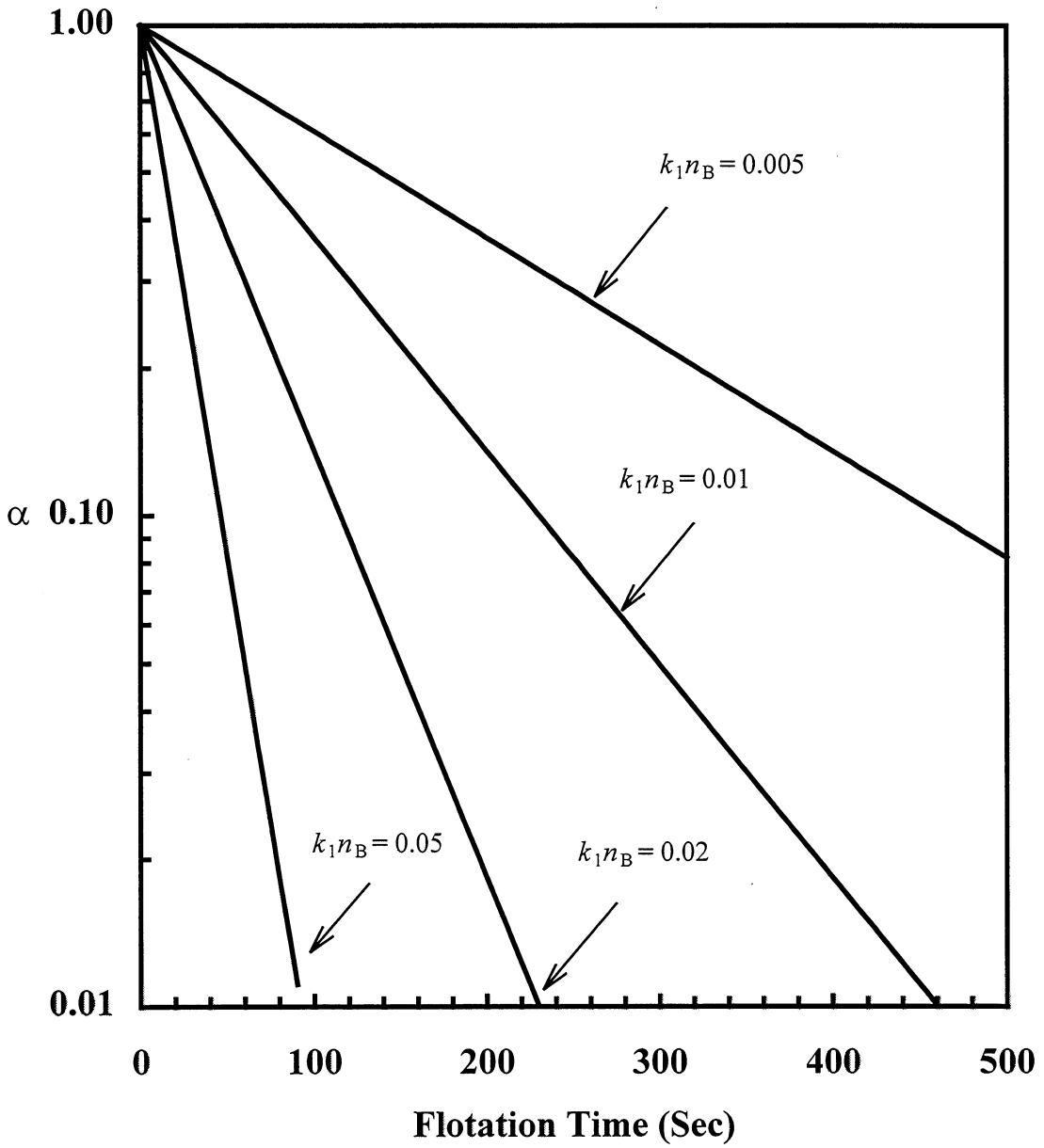

Figure 2: Concentration of ink particles in the flotation accepts as a function of time.

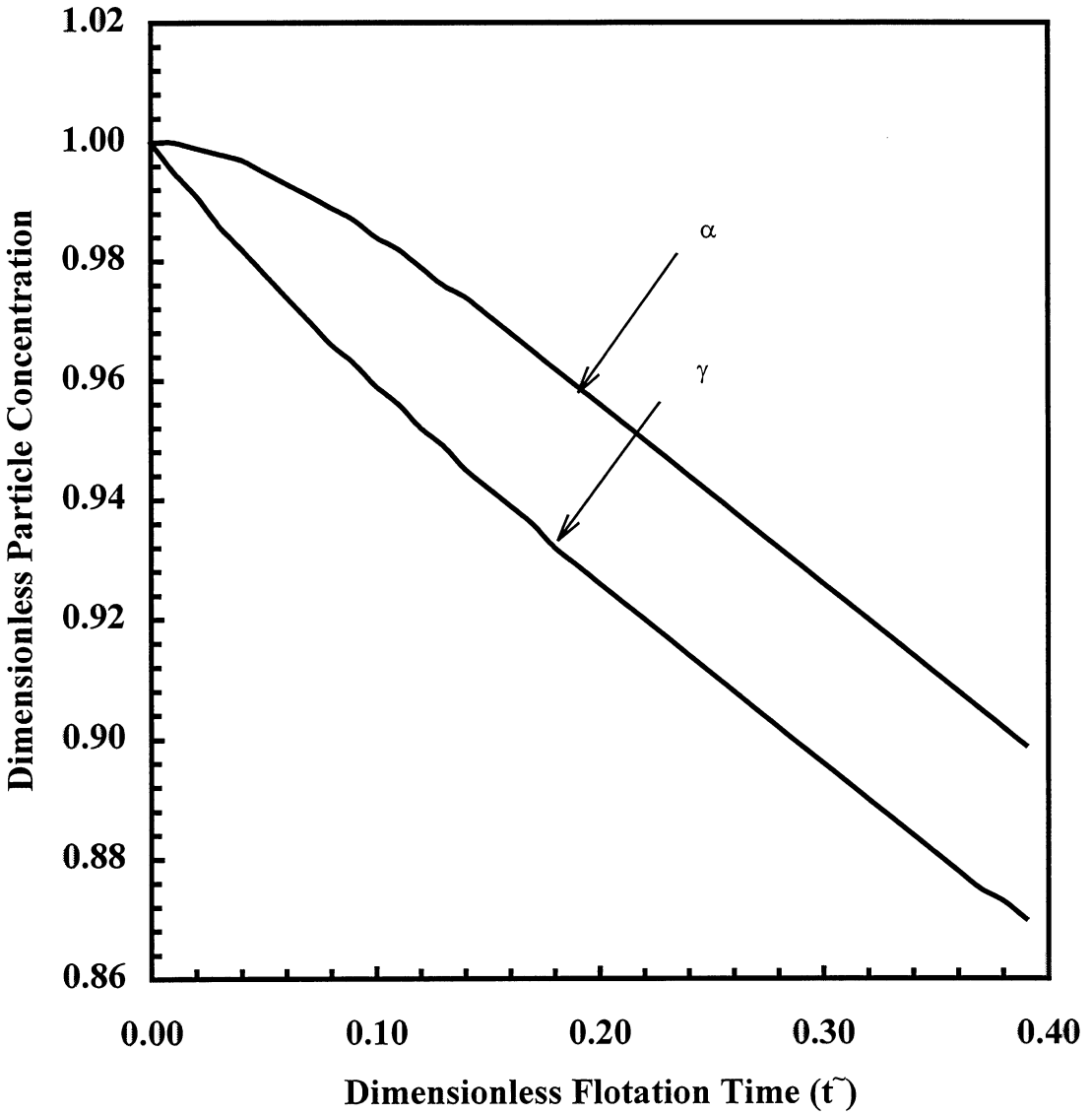

Figure 3: Initial decay of total (α) and free (γ) particles as a function of non-dimensional time ($\varepsilon_p = 0.1$, $\tilde{k_1} = 10^{-1}$, $\tilde{k_2} = 10^{-2}$, $n_B = 1.0$ /cm^3, $n_{po}^f = 10$ / cm^3, $t^* = 5$s).

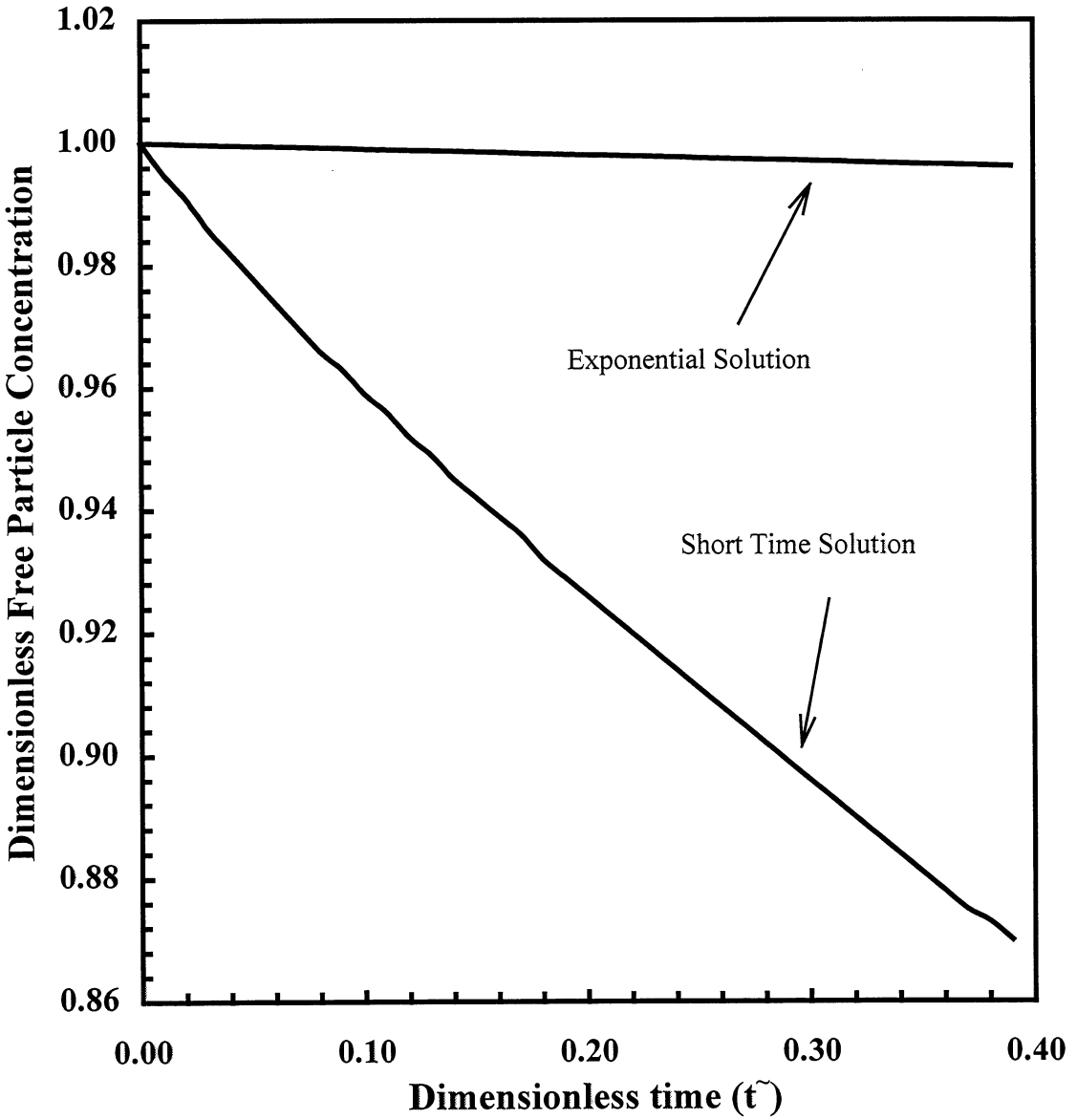

Figure 4: Comparison of the exponential solution with the short time solution valid for initial times ($\varepsilon_p = 0.1$, $\tilde{k}_1 = 10^{-1}$, $\tilde{k}_2 = 10^{-2}$, $n_B = 1.0$ /cm^3, $n_{po}^f = 10$ /cm^3, $t^* = 5$s).

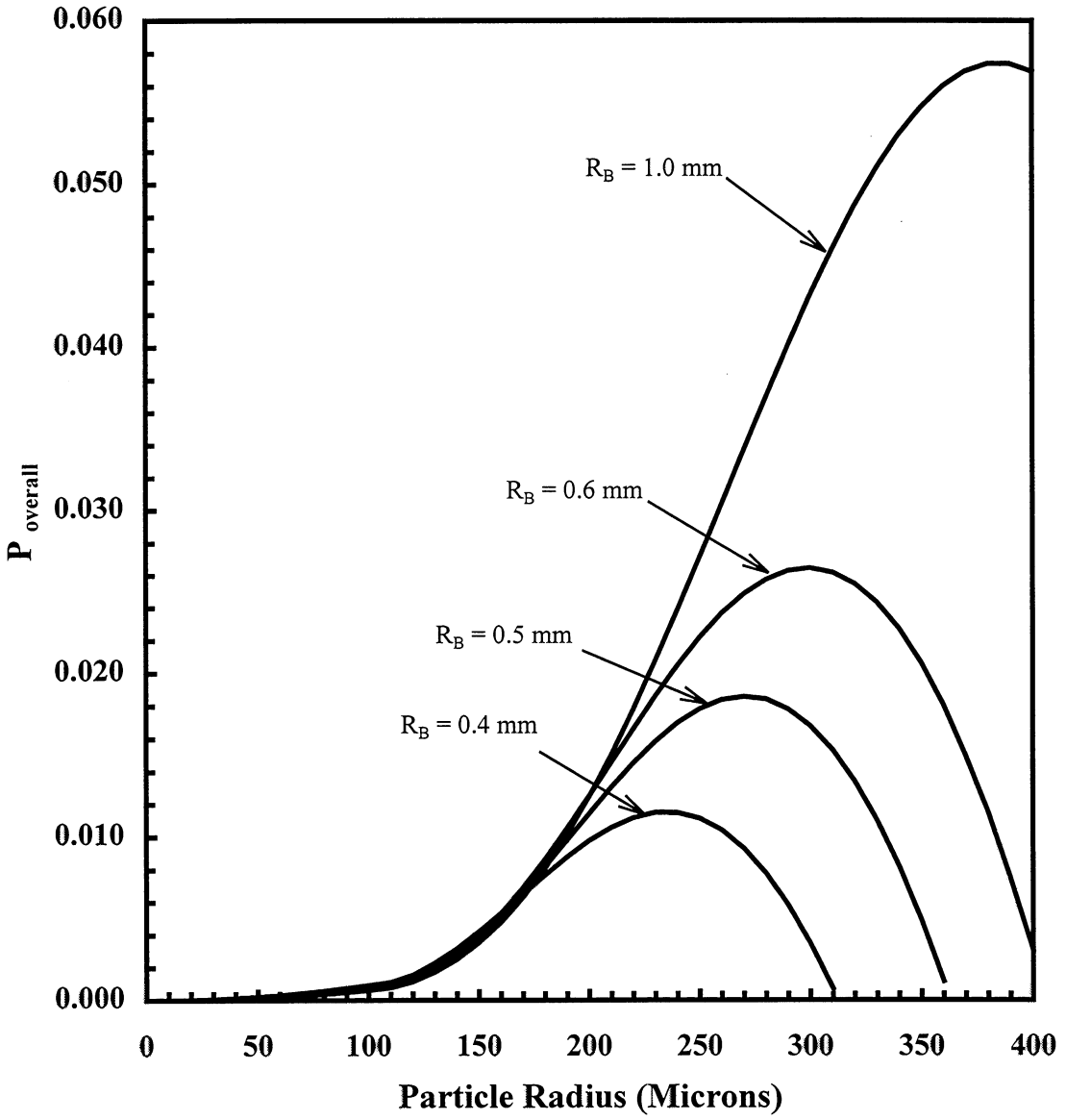

Figure 5: Overall probability of the formation of a bubble/particle aggregate as a function of particle radius.

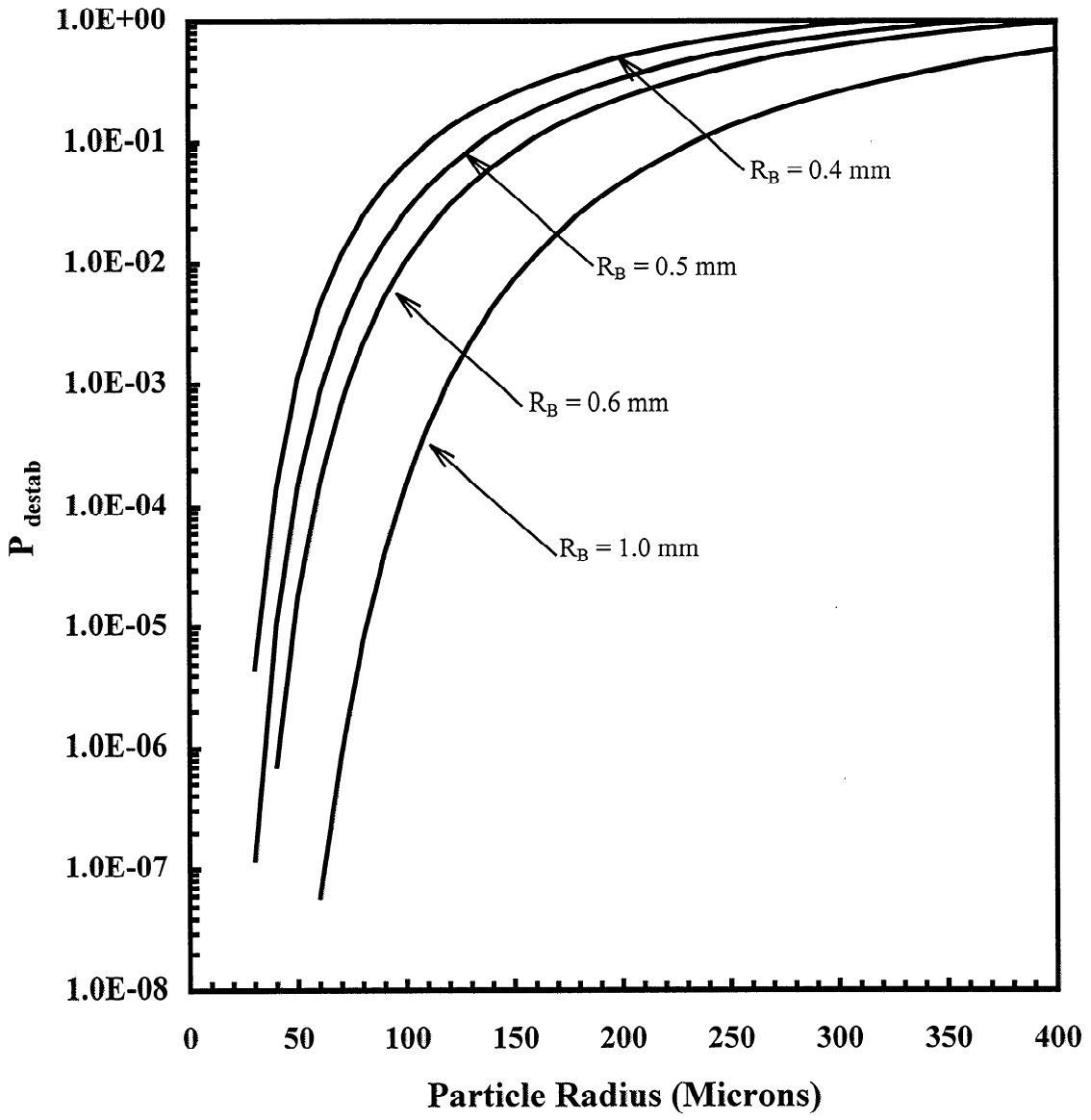

Figure 6: Probability of destabilization of a bubble/particle aggregate as a function of particle radius.

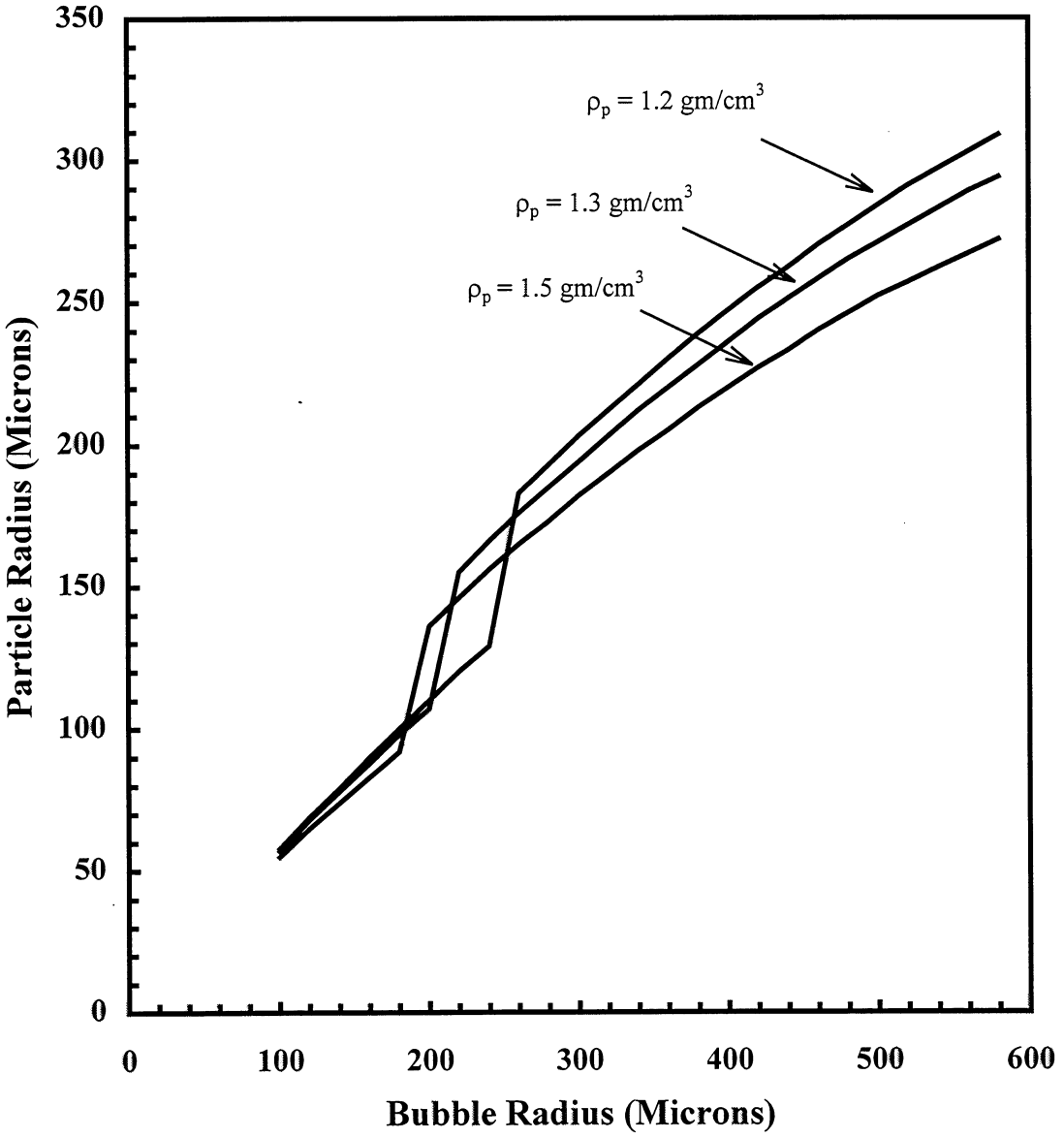

Figure 7: Particle radius as a function of the bubble radius for which the overall probability of bubble/particle aggregate formation is highest.